CSMA 2022
15ème Colloque National en Calcul des Structures
16-20 Mai 2022, Presqu'île de Giens (Var)

Robustness and weak scalability assessment of a preconditioner for coupled Thermo-Hydro-Mechanics problems

A. Ordonez[1], N. Tardieu[1], C. Kruse[2], D. Ruiz[3]

[1] *EDF/R&D, IMSIA UMR EDF-CNRS-CEA-ENSTA 9219, Palaiseau {ana-clara.ordonez-egas,nicolas.tardieu}@edf.fr*
[2] *Cerfacs, Toulouse, carola.kruse@cerfacs.fr*
[3] *Institut National Polytechnique, Toulouse, daniel.ruiz@toulouse-inp.fr*

Abstract — We are interested in the modelling of coupled thermo-hydro-mechanical (THM) problems that describe the behaviour of a soil in which a weakly compressible fluid evolves. It is used for the evaluation of the THM impact of high-level activity radioactive waste exothermicity within a deep geological disposal facility. We shall present the definition of a block preconditioner for the fully coupled THM equations. Numerical results reflect the good performance of the proposed preconditioner that shows to be weakly scalable until more than 2000 cores and more than 1 billion degrees of freedom.
Mots clés — Multiphysics, Preconditioning, Biot's Problem, Finite Elements, HPC.

1 Introduction

1.1 Context

The detailed modeling of underground phenomena is of major interest in several industrial fields ranging from oil and gas to nuclear waste storage and civil engineering. This is particularly the case for coupled phenomena where several physics come into play and can make it difficult to understand their respective influences.
The modeling of underground phenomena has been initiated by the pioneering work of Terzaghi in his theory of one-dimensional consolidation [1]. The theory was then expanded by Biot, who used the coupling of Darcy's and Hooke's laws together with the Terzaghi's principle [2]. Then, he also included the effect of temperature by using the new concept of "virtual dissipation" [3]. Finally Coussy showed that a general theory of thermomechanics of saturated porous media could be established based on standard thermodynamics principles [4].
Coupled thermo-hydo-mechanics (THM) is the topic of this communication, with special attention to numerical implementation and scalable parallel solvers.

1.2 The THM equations

An isotropic incompressible saturated mono-phased porous media is considered ; it is modeled as a solid skeleton containing fluid filled pores. The essential parameters of the medium are :

- the porosity, named ϕ in the sequel. It is the ratio between the volume of the void and the total volume of the medium,
- the intrinsic permeability named K_{int}. It measures the material's ability to transmit fluids, with λ^H, the hydraulic permeability, being a function of it,
- the thermal conductivity named λ^T. It measures the medium's ability to conduct heat.

Other parameters worthwhile mentioning are :

- the Biot's coefficient b but since the medium is incompressible it will translate into $b = 1$,
- the saturation named S, that describes the moisture content of the medium who will also be $S = 1$ because the medium is saturated.

- the volumetric enthalpy of the water has been neglected in order to simplify the energy conservation equation. It is a strong simplification but it does not compromise the preconditioning strategy in the general case.

These parameters, some of which appear explicitly therein, are of major importance in the balance equations. They are three in number since the medium is saturated and mono-phased : the mechanics equilibrium equation, the water mass conservation and the energy conservation. After detailing each balance equation in order to reveal the detailed coupling between the phenomena involved, the final system is obtained.

Let Ω be a d dimensional domain, $1 \leq d \leq 3$, and t_f the final time of the simulation. The THM model describes the evolution of 3 primal unknowns. The vector displacement field, $\underline{u}(x,t)$, the fluid pressure field, $p(x,t)$, the temperature field $T(x,t)$.

The coupled system consists of , $\forall x \in \Omega$ and $\forall t > 0$:

$$-\operatorname{div}(\underline{\underline{A}} : \underline{\underline{\varepsilon}}(\underline{u})) + \nabla p + 3K\alpha_s \nabla T = \underline{f}^e \qquad \text{in } \Omega \times (0,t_f)$$

$$-\rho_f \operatorname{div}(\lambda^H \nabla p) + \rho_f \left(\operatorname{div}(\dot{\underline{u}}) + \frac{\phi}{K_l}\dot{p} - \alpha_m 3\dot{T} \right) = g^e \qquad \text{in } \Omega \times (0,t_f)$$

$$-\operatorname{div}(\lambda^T \nabla T) + (3K_0\alpha_s \operatorname{div}(\dot{\underline{u}}) - 3\alpha_m \dot{p} - 9K_0\alpha_s^2 \dot{T})T_0 + C_\sigma^0 \dot{T} = \Theta \qquad \text{in } \Omega \times (0,t_f)$$

where $\underline{f}^e$ denotes the total volume external forces, g^e the total fluid sources and Θ the total sources of heat. It is worth noticing the use of the Hooke's, Darcy's and Fourier's laws in the above equations.
The boundary of Ω is denoted $\partial\Omega$ and 6 different partitions are needed to define the boundary conditions. For each primal unknown, we may define Dirichlet and Neumann boundary conditions, say the displacement $\underline{u}$ and the stress $\underline{\underline{\sigma}}$, the pressure p and the fluid flux ζ, the temperature T and the thermal flux Φ.
We thus have, respectively, the boundary conditions on the displacement unknowns, on the pressure unknowns and on the temperature unknowns such as :

$$\partial\Omega = \partial\Omega^{\underline{u}} \cup \partial\Omega^{\underline{\underline{\sigma}}} \text{ with } \partial\Omega^{\underline{u}} \cap \partial\Omega^{\underline{\underline{\sigma}}} = \emptyset$$
$$\partial\Omega = \partial\Omega^{p} \cup \partial\Omega^{\zeta} \text{ with } \partial\Omega^{p} \cap \partial\Omega^{\zeta} = \emptyset$$
$$\partial\Omega = \partial\Omega^{T} \cup \partial\Omega^{\Phi} \text{ with } \partial\Omega^{T} \cap \partial\Omega^{\Phi} = \emptyset$$

The boundary conditions are given by :

$$\begin{aligned}
\underline{\underline{\sigma}}(\underline{u}) \cdot \underline{n} &= \underline{t}^e && \text{on } \partial\Omega^{\underline{\underline{\sigma}}} \times (0,t_f) \\
-\lambda^H \nabla p \cdot \underline{n} &= \zeta^e && \text{on } \partial\Omega^{\zeta} \times (0,t_f) \\
-\lambda^T \nabla T \cdot \underline{n} &= \Phi^e && \text{on } \partial\Omega^{\Phi} \times (0,t_f) \\
\underline{u} &= \underline{u}^e && \text{on } \partial\Omega^{\underline{u}} \times (0,t_f) \\
p &= p^e && \text{on } \partial\Omega^{p} \times (0,t_f) \\
T &= T^e && \text{on } \partial\Omega^{T} \times (0,t_f) \\
\underline{u}(,0) &= \underline{u}_0 && \text{in } \Omega \\
p(,0) &= p_0 && \text{in } \Omega \\
T(,0) &= T_0 && \text{in } \Omega
\end{aligned}$$

where $\underline{n}$ is the outward normal.
Furthermore, the material parameters' definitions are given in Table 1.

We use the implicit Euler method for time discretization and the finite element method with Taylor-Hood P2-P1-P1 elements for space discretization. This translates into using continuous piecewise quadratics to approximate the displacement and continuous piecewise linears to approximate the pressure and

Table 1: Parameters

Symbol	Definition	Unit
$\underline{\underline{A}}$	Forth order Hooke's tensor	Pa
$\underline{\underline{\varepsilon}}$	Strain tensor	-
E	Young's modulus	Pa
ν	Poisson's ratio	-
K	Bulk modulus of the solid	Pa
K_0	"Drained" bulk modulus of the medium	Pa
K_l	Bulk modulus of the fluid	Pa
ϕ	Porosity	-
μ_l	Fluid dynamic viscosity	Pa.s
C_s	Specific heat of the solid	$J.kg^{-1}.K^{-1}$
C_f	Specific heat of the fluid	$J.kg^{-1}.K^{-1}$
C_σ^0	Homogenized specific heat of the medium	-
ρ_s	Solid density	$kg.m^{-3}$
ρ_f	Fluid density	$kg.m^{-3}$
ρ_m	Medium density	$kg.m^{-3}$
λ^H	Hydraulic conductivity	$Pa^{-1}.m^2.s^{-1}$
λ^T	Thermal conductivity	$W.m^{-1}.K$
T_0	Temperature of reference	K
α_s	Dilation coefficient of the solid	K^{-1}
α_l	Dilation coefficient of the fluid	K^{-1}
α_m	Homogenized dilation coefficient of the medium	K^{-1}

the temperature. In [5], these elements where studied for poroelasticity and having the polynomial interpolation for the displacement be one degree higher than for the pressure, equilibrates the convergence rate of all terms in the energy norm. Furthermore the convergence is robust with respect to the mesh size.

2 The preconditioner

When considering the preconditioning of coupled multi-physics problems, two approaches are highlighted in the literature:

- Block preconditioners with a multigrid preconditioning inside each block [6],
- Multigrid algorithm with block preconditioners as smoothers [7].

The former approach is the route that we took for convenience with respect to integration into code_aster.

All the solvers presented use a preconditioned FGMRES method [8] with the notation: FGMRES(A,P), where A is the system to solve, and P the preconditioner. For P, a Block Gauss-Seidel preconditioner was chosen. It is implemented in PETSc as follows:

$$P^{-1} = \begin{bmatrix} \tilde{A}_{\underline{u}\underline{u}}^{-1} & 0 & 0 \\ 0 & \boldsymbol{I}_d & 0 \\ 0 & 0 & \boldsymbol{I}_d \end{bmatrix} \begin{bmatrix} \boldsymbol{I}_d & -A_{\underline{u}p} & -A_{\underline{u}T} \\ 0 & \boldsymbol{I}_d & 0 \\ 0 & 0 & \boldsymbol{I}_d \end{bmatrix} \begin{bmatrix} \boldsymbol{I}_d & 0 & 0 \\ 0 & \tilde{A}_{pp}^{-1} & 0 \\ 0 & 0 & \boldsymbol{I}_d \end{bmatrix} \begin{bmatrix} \boldsymbol{I}_d & 0 & 0 \\ 0 & \boldsymbol{I}_d & -A_{pT} \\ 0 & 0 & \boldsymbol{I}_d \end{bmatrix} \begin{bmatrix} \boldsymbol{I}_d & 0 & 0 \\ 0 & \boldsymbol{I}_d & 0 \\ 0 & 0 & \tilde{A}_{TT}^{-1} \end{bmatrix}$$

where $\tilde{A}_{**}^{-1} = \text{FGMRES}(A_{**}, \text{Boomer})$ or $\tilde{A}_{**}^{-1} = \text{MUMPS}(A_{**})$. Boomer refers to the algebraic multigrid preconditioner BoomerAMG of the Hypre library and MUMPS to the MUltifrontal Massively Parallel Solver [10][9].
The stopping criteria of FGMRES is the relative convergence tolerance that was set to 10^{-6}. In addition, when solving $\tilde{A}_{\underline{u}\underline{u}}^{-1}$ with FGMRES the maximum number of iteration was set to 10, for $\tilde{A}_{pp}^{-1}$ it was set to 20 and for $\tilde{A}_{TT}^{-1}$ to 11.

3 Results

We now turn to the presentation of a test case with results using the block Gauss-Seidel preconditioner where each diagonal block is solved using a FGMRES method preconditioned by Boomer. The method is implemented in code_aster, the massively parallel open source general purpose finite element solver developed at EDF R&D [12].

3.1 Test case in code_aster

The test case needs to be simple enough so that the mesh can be easily refined but complex enough to resemble the industrial problem in consideration.

To do so, a bi-material example was chosen. It is a 3D rectangular box as seen in figure 1, with a 0.1 m length following x, a 0.1 m height following y and 0.05 m large following z. The tetrahedral mesh was generated using Gmsh 4.4.1.

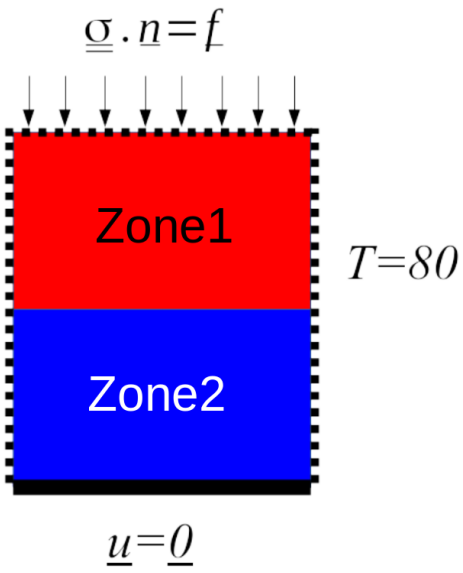

Figure 1: Bi-material test case

Table 2: The test case parameters

Medium	Value
μ_l	10^{-3}
K_l	2.10^9
C_s	1000
C_f	4180
ρ_f	1000
λ^T	1.6
T_0	273
α_s	10^{-5}
α_l	10^{-4}
K_0	K
λ^H	K_{int}/μ_l
C^0_σ	$C_s\rho_s(1-\phi)+C_l\rho_f\phi$
ρ_s	$(\rho_m-\phi\rho_f)/(1-\phi)$
α_m	$\phi\alpha_l+(1-\phi)\alpha_s$

Clay	Value
E	6.10^9
ν	0.3
ρ_m	2410
K_{int}	4.10^{-21}
ϕ	0.18

Concrete	Value
E	15.10^9
ν	0.2
ρ_m	2500
K_{int}	10^{-11}
ϕ	0.2

In Figure 2, Zone 1 is made of clay and Zone 2 is made either of clay or of concrete. The value of the parameters,displayed in Table 2, are realistic and represent the type industrial problems in consideration [11]. The displacement was set to 0 on the bottom surface (y=0), a mechanical pressure was applied

on the top surface (y=0.1) and an 80 °C temperature was set on the whole surface of the sample. The tests were solved with code_aster using the THM framework presented in the section above, an isotropic saturated mono-phased THM medium using P2-P1-P1 finite elements.

3.2 Parameter sensibility

One of the biggest issue when solving the THM system is the variety of parameters and the sometimes huge difference in orders of magnitude. We start by measuring the impact of parameters that can have different sets of values by changing the Young's modulus, the intrinsic permeability and the thermal conductivity. We have chosen to vary these parameters since each of them appears respectively in each balance equation and since they have a major influence therein. The tests are done using the test case of Figure 2 with Zone 1 and Zone 2 made of clay, using the medium and clay parameters from Table 2.

For each set of parameters and mesh fineness, we give the number of outer FGMRES iterations followed by the condition number of the preconditioned system in parentheses. The results are compiled in Table 3.

Table 3: Parameter robustness

Parameters			Dof		
E	Intr. Perm.	Therm. Cond.	10 000	60 000	1 500 000
1.0e+09	4.0e-15	4.0e-01	4 (56)	5 (65)	5 (74)
		2.3e+00	4 (57)	4 (72)	5 (87)
	4.0e-18	4.0e-01	5 (108)	6 (82)	6 (74)
		2.3e+00	5 (116)	5 (93)	5 (88)
	4.0e-21	4.0e-01	21 (53)	22 (100)	20 (408)
		2.3e+00	18 (54)	20 (111)	17 (357)
2.5e+10	4.0e-15	4.0e-01	5 (12)	6 (6)	6 (3)
		2.3e+00	5 (2)	5 (2)	5 (2)
	4.0e-18	4.0e-01	5 (12)	6 (6)	6 (3)
		2.3e+00	5 (2)	5 (2)	5 (2)
	4.0e-21	4.0e-01	8 (16)	8 (12)	8 (4)
		2.3e+00	7 (12)	7 (9)	7 (4)
5.0e+10	4.0e-15	4.0e-01	5 (18)	6 (8)	6 (2)
		2.3e+00	5 (2)	5 (2)	5 (1)
	4.0e-18	4.0e-01	5 (18)	6 (8)	6 (2)
		2.3e+00	5 (2)	5 (2)	5 (1)
	4.0e-21	4.0e-01	7 (13)	7 (8)	7 (3)
		2.3e+00	6 (6)	6 (3)	6 (2)

It is worth mentioning the very large range of variation of mesh fineness and of each parameter (up to 6 orders of magnitude). When analysing Table 3, the first point to highlight is the excellent independence to mesh size : in each line, the outer number of FGMRES iteration remains constant. Then, looking at the results in column, we note a moderate variation of this number, that remains mostly under 10 except for the "worst" set of parameters (low E and low K_{int}), where it only reaches 20. In this case nevertheless, the number of internal FGMRES iterations remains as low as 10 for the displacement block and 6 for the pressure and temperature blocks. We conclude that the proposed preconditioner behaves well on these large ranges of variation, making the condition number of the preconditioned system vary from 2 to 400.

3.3 Weak scalability

The weak scalability of the preconditioner is evaluated on the previous test case. EDF's cluster Cronos was used to run the scalability tests. It has 2 Xeon Platinum 8260 24C 2.4GHz processors per node. Each CPU is equipped with 24 cores .

A weak scalability test consists in setting a fixed number of degree of freedom (Dof) by processor and increasing the size of the problem by increasing the number of processes. In other words, we set the size of a sub-domain and make the problem bigger by increasing the total number of sub-domains. Our goal is to investigate if the solution algorithm needs the same resolution time whether we solve N Dof on 1 process or 1000xN Dof on 1000 processes. In case of perfect weak scalability, the time should remain constant when increasing the number of processes. Realistic parameters where chosen for the weak scalability test. The bi-material case from Figure 2 was chosen for the weak scalability test, with Zone 1 made of clay and Zone 2 made of concrete using the parameters values from Table 2.

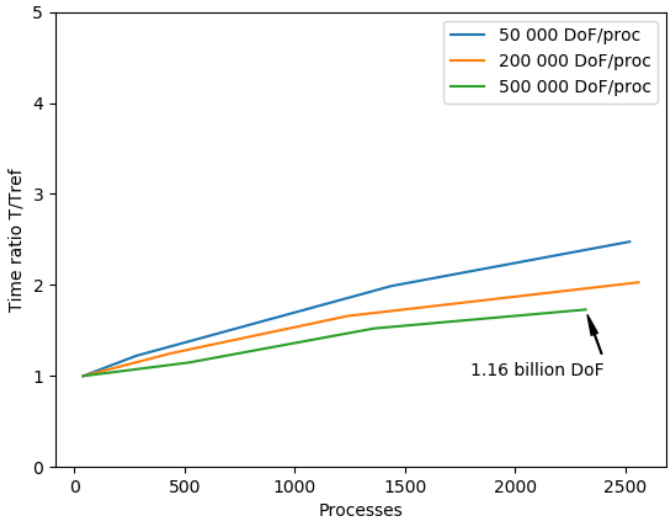

Figure 2: Time ratio as a function of the number of processes

As can be seen in the Figure 2, the number of Dof per process was fixed to 50 000 (blue line), 200 000 (orange line) and 500 000 (green line) and the test case was run of 40 processes to 2500 processes. The ratio between the solution time to the 40 processes time is presented.

For small numbers of Dof per process, it remains between 1. and 2.5 times the initial time, whereas for 500 000, it remains between 1. and 1.7. We highlight that the size of the linear system ranges from 20 million to more than 1 billion Dof. This sub-optimal behavior for small sub-domains is often due to latency of the cluster's network. When sub-domains are large and there is more work per process, the computation dominates the cost associated with communication. This is a very good scalability result since the test case is rather complex especially due to the variation of material parameters between clay and concrete.

4 Conclusion

In this communication is presented the assessment of the robustness and the weak scalability of a preconditioner dedicated to coupled THM problems. A simple yet representative test case has been set up, on which the preconditioner shows excellent mesh size independence, good robustness with respect to parameters variation and good weak scalability.

Though established in the linear regime, these results a very valuable when considering to move to nonlinear constitutive laws. This point is being investigated and encouraging results have already been obtained.

References

[1] K. Terzaghi. *Erdbaumechanik auf bodenphysikalischer grundlage*, Leipzig u, Wien: F. Deuticke, 1925.

[2] M.A. Biot. *General Theory of Three-Dimensional Consolidation*, Journal of Applied Physics 12, 155-164, 1941.

[3] M.A. Biot. *Variational Lagrangian-thermodynamics of nonisothermal finite strain mechanics of porous solids and thermomolecular diffusion*, International Journal of Solids and Structures, Volume 13, Issue 6, 579-597, 1977.

[4] O. Coussy. *A general theory of thermoporoelastoplasticity for saturated porous materials*, Transport in Porous Media 4, 281–293, 1989.

[5] A. Ern, S. Meunier. *A posteriori error analysis of Euler-Galerkin approximations to coupled elliptic-parabolic problems*, ESAIM: Mathematical Modelling and Numerical Analysis 43, 353–375,2009.

[6] H. Elman, D. Silvester, and A. Wathen. *Finite Elements and Fast Iterative Solvers: With Applications in Incompressible Fluid Dynamics*, Numerical Mathematics and Scientific Computation Oxford University Press, 2006.

[7] F.J. Gaspar, C. Rodrigo. *On the fixed-stress split scheme as smoother in multigrid methods for coupling flow and geomechanics*, Computer Methods in Applied Mechanics and Engineering, 526–540, 2017.

[8] Y. Saad. *A Flexible Inner-Outer Preconditioned GMRES Algorithm*, SIAM J. Sci. Comput 14, 461-469,1993.

[9] P.R. Amestoy , I. S. Duff, J. Koster, J.-Y. L'Excellent. *A Fully Asynchronous Multifrontal Solver Using Distributed Dynamic Scheduling*, SIAM Journal on Matrix Analysis and Applications 23, 15-41, 2001.

[10] R. Falgout, J. Jones,U. Yang. *The Design and Implementation of hypre, a Library of Parallel High Performance Preconditioners*, Lecture Notes in Computational Science and Engineering 51, 267-294, 2006.

[11] R. Giot, S. Granet, M. Faivre, N. Massoussi, J. Huang. *A transversely isotropic thermo-poroelastic model for claystone: parameter identification and application to a 3D underground structure*, Geomechanics and Geoengineering, 246-263, 2018.

[12] code_aster web site. `http://www.code-aster.org`